

Intracellular order formation through stepwise phase transitions

Yuika Ueda¹ and Shinji Deguchi^{1,*}

¹ Division of Bioengineering, Graduate School of Engineering Science, Osaka University

* Corresponding author

Address: 1-3 Machikaneyama, Toyonaka, Osaka 560-8531, Japan

E-mail: deguchi.shinji.es@osaka-u.ac.jp

Phone: +81 6 6850 6215

ORCID: 0000-0002-0556-4599

Abstract

Living cells inherently exhibit the ability to spontaneously reorganize their structures in response to changes in both their internal and external environments. Among these responses, the organization of stress fibers composed of actin molecules changes in direct accordance with the mechanical stiffness of their environments. On soft substrates, SFs are rarely formed, but as stiffness increases, they emerge with random orientation, progressively align, and eventually form thicker bundles as stiffness surpasses successive thresholds. These transformations share similarities with phase transitions studied in condensed matter physics, yet despite extensive research on cellular dynamics, the introduction of the statistical mechanics perspective to the environmental dependence of intracellular structures remains underexplored. With this physical framework, we identify key relationships governing these intracellular transitions, highlighting the delicate balance between energy and entropy. Our analysis provides a unified understanding of the stepwise phase transitions of actin structures, offering new insights into related biological mechanisms. Notably, our study suggests the existence of “mechanical” checkpoints in the G1 phase of the cell cycle, which sequentially regulate the formation of intracellular structures to ensure proper cell cycle progression.

Keywords: substrate stiffness, phase transition, statistical mechanics, thermodynamics, mechanobiology, self-assembly, cell spreading

Introduction

Living cells inherently exhibit the ability to adaptively modify their structures in response to changes in both their internal and external environments. Among these responses, cells adjust the formation of actin contractile bundles, or stress fibers (SFs), in accordance with the stiffness of their environment. Interestingly, the extent and organization of SFs within cells depend on the stiffness of the extracellular substrate (1). On significantly soft substrates, SFs are hardly formed, but once the substrate stiffness exceeds a certain threshold, they form but remain randomly oriented (2). On substrates with greater stiffness, relatively thin SFs begin to align in the same direction, and beyond an even higher stiffness threshold, these aligned SFs come into close proximity and register laterally with one another, forming thicker actine bundles (3). These stepwise transformations in the organization of SFs are also observed in succession when cells are plated on sufficiently stiff substrates (4–6). As these adaptive changes occur spontaneously in accordance with the level of substrate stiffness, cells exhibit characteristics reminiscent of phase transitions in physics.

Phase transitions occur when a stable phase of a system shifts due to environmental changes, altering macroscopic properties without changes to internal components. These significant changes, driven by variations in internal and external parameters, have been a central focus in the statistical mechanics of systems, particularly in condensed matter physics (7). The concept of phase transitions has even been extended to biological phenomena at the cellular level, especially in the context of phase separation. However, the stepwise transitions in intracellular actin organization in response to substrate stiffness remain underexplored from this perspective, despite their apparent relevance. Given that substrate stiffness significantly influences cellular behaviors such as proliferation, differentiation, and apoptosis, namely key areas of mechanobiology research over the past two decades, uncovering the inherent principles that dictate the inevitable emergence of intracellular reorganization could provide new insights into the physical environment-dependent nature of living cells.

Here we aim to describe the physical mechanisms underlying the stepwise phase transitions using the framework of statistical mechanics. By focusing on the spatial arrangement of actin molecules in a cell lattice model, we derive the essential conditions leading to transitions between different macroscopic cell phases with distinct microscopic SF organizations. Although our simplified models only implicitly consider the involvement of other factors such as myosin molecules, this approach provides a theoretical basis for understanding the environment-driven cellular adaptive mechanisms.

Model overview

Cells undergo stepwise phase transitions in accordance with the magnitude of substrate stiffness (Fig. 1) (8). Specifically, i) on the softest substrates, actin particles considered as the fundamental units of SFs in our model are randomly distributed within the cell; ii) as substrate stiffness increases, these particles are allowed to aggregate into SFs, while their orientation remains random; iii) upon reaching a higher threshold of stiffness, SFs align uniformly in a single direction; and iv) when the substrate stiffness surpasses another critical threshold, these aligned SFs undergo interfibre coalescence. Thus, substrate stiffness dictates that cells adopt specific actin patterns or phases. This plastic phase transitions reflect a key characteristic of cellular adaptation to varying environmental conditions. To explain the physical necessity underlying these transitions, we consider four distinct phases, each characterized by a different nature of cellular "order." A key challenge lies in defining what constitutes the specific order that characterizes the cell interior in each phase. While conventional phase transition theories typically focus on a single order parameter, the current cellular phenomena involve a hierarchy of phase transitions, each with its own distinct form of an order that is inherited by subsequent phases. We describe the emergence and loss of multiple orders within cells upon specific thresholds of environmental stiffness.

Phase transition 1

We begin by considering the phase transition process, in which randomly distributed actin particles form SFs, characteristic of Phase transition 1 (PT1). The cell is represented as a two-dimensional square with a side length of a , on which actin particles are distributed (Fig. 2). We assume that the cell does not undergo work or energy changes associated with shape or volume alterations, even though actual cells do experience such changes. We are interested in the spontaneous phenomena that occur independently of macroscopic geometric alterations. We also assume that the temperature of the cell remains constant. The Helmholtz free energy of the cell is defined as follows:

$$A = E - TS \quad (1 - 1)$$

where E , T , and S represent energy, temperature, and entropy, respectively. We derive the specific form of Eq. (1-1) by considering the distribution of actin particles. The square cell is subdivided into smaller units referred to as a lattice. The total number of lattice sites is equal to the area of the cell V :

$$V = a^2 \quad (1 - 2).$$

Let N_a represent the total number of actin particles within the cell, which remains constant as actin works as a "housekeeping" protein. The cell is sufficiently large relative to the area occupied by all actin particles to ensure $N_a < V$, and each lattice site can be occupied by at most one actin particle.

We define SFs as the arrangement of actin particles that align in a straight line from one edge of the cell to the other (Fig. 2, red). Any other configurations are considered to be randomly distributed actin particles (Fig. 2, green). Although SFs in actual cells may not always form perfect straight lines, we define SFs in this way to enable a strict count of the possible microscopic states, or microstates, of this macroscopic cell system. Here note that, in statistical mechanics systems such as those applied to biological contexts (9–13), the distinction between macroscopic and microscopic variables is not simply determined by physical size. In the case of a protein statistical mechanics, for example, countable degrees of freedom typically include the length of the protein chain, while uncountable degrees of freedom would refer to the relative coordinates of individual atoms within the protein structure. In addition, while SFs in real cells can vary in length and do not necessarily span the entire cell, we consider the length a in our lattice model as the minimum length required to count as an SF. For more complex cases with varying SF lengths, the current system may be seen as a sub-system of the cell, but such analyses are beyond the scope of this study, which focuses on the essential aspects of the phenomena.

Let L_s represent the number of SFs formed by actin particles. To characterize the phase state, we define an order parameter, which is a macroscopic variable that determines the degree of order within the cell, based on the extent to which SFs are formed. Specifically, the order parameter x_1 is defined as the ratio of actin particles involved in SF formation to the total number:

$$x_1 = \frac{L_s a}{N_a} \quad (1 - 3)$$

When $x_1 = 0$, no SFs are formed, indicating a completely disordered state. Meanwhile, when $x_1 = 1$, all actin particles form SFs, representing a fully ordered state within the cell. We determine the specific form of the entropy by counting the possible microstates. Actin particles can exist in two distinct states: as part of non-SFs or as part of SFs. First, the number of possible microstates of actin particles or non-SFs (Fig. 2, green) is given by:

$$W_p = \frac{(V - L_s a)!}{(N_a - L_s a)! (V - N_a)!} \quad (1 - 4)$$

where the available lattice sites are those not involved in SF formation (i.e., $V - L_s a$), and the number of available actin particles and empty lattice sites are $N_a - L_s a$ and $V - N_a$, respectively. Similarly, the number of possible microstates of SFs (Fig. 2, red) is given by

$$W_s = \frac{2a!}{L_s! (2a - L_s)!}, \quad (1 - 5)$$

in which the number of possible configurations is calculated for arranging a total of L_s SFs. We do not distinguish between SF configurations that are symmetrical with respect to the starting position, either vertically or horizontally. The number of possible microstates is thus calculated within the range of $a + a = 2a$. Taken together, the system entropy is described, with the Stirling approximation, by

$$\begin{aligned} S_1 &= k_b \ln W_p W_s \\ &= k_b \left\{ \begin{aligned} &(V - N_a x_1) \ln(V - N_a x_1) - N_a(1 - x_1) \ln N_a(1 - x_1) - (V - N_a) \ln(V - N_a) \\ &+ 4a \ln a - 2a \ln 2 - \frac{N_a}{a} x_1 \ln N_a x_1 - \left(2a - \frac{N_a}{a} x_1\right) \ln(2V - N_a x_1) \end{aligned} \right\} \quad (1 - 6) \end{aligned}$$

where k_b is the Boltzmann constant (Fig. S1).

Next, to describe the energy E_1 , we define the single-particle energy of an actin particle as μ_1^0 and the interaction energy due to binding as μ_1^s , respectively; μ_1^0 is an intrinsic energy that reflects the inherent properties of the actin particle and is considered a constant, while μ_1^s represents the energy associated with the stability of the binding and is generally a function that can vary depending on chemical and physical influences from the surrounding environment. Given that actin–myosin complexes including SFs become more stable as the sustained tension increases, a property known as a catch bond (14–18), the interaction energy is expressed as a function of the tension F_1 :

$$\mu_1^s(F_1) = B \exp(-CF_1) \quad (1 - 7)$$

where B is the interaction energy due to binding in the absence of tension, and C is the constant that determines the effect of F_1 . The total energy of the cell is expressed using the number of non-SF actin particles, $N_a - L_s a$, and the number of particles forming SFs, L_s (Fig. S2):

$$E_1 = \mu_1^0(N_a - L_s a) + \mu_1^s L_s a \quad (1-8)$$

From Eqs. (1-6) and (1-8), the free energy of Eq. (1-1) is expressed as

$$A_1 = \mu_1^0(N_a - x_1 N_a) + B N_a x_1 \exp(-C F_1) - T k_b \left\{ \begin{aligned} & (V - N_a x_1) \ln(V - N_a x_1) - N_a(1 - x_1) \ln N_a(1 - x_1) - (V - N_a) \ln(V - N_a) \\ & + 4a \ln a - 2a \ln 2 - \frac{N_a}{a} x_1 \ln N_a x_1 - \left(2a - \frac{N_a}{a} x_1\right) \ln(2V - N_a x_1) \end{aligned} \right\}. \quad (1-9)$$

To derive the conditions for PT1, we take the partial derivative of Eq. (1-9) with respect to x_1 :

$$\frac{\partial A_1}{\partial x_1} = N_a \left[(\mu_1^s - \mu_1^0) - k_b T \left\{ -\ln(V - N_a x_1) + \ln N_a(1 - x_1) - \frac{1}{a} \ln N_a x_1 + \frac{1}{a} \ln(2V - N_a x_1) \right\} \right] \quad (1-10)$$

The order parameter x_1^* that satisfies $\partial A_1 / \partial x_1 = 0$ is

$$x_1^* \approx 1 - \frac{V}{N_a} \exp \frac{\mu_1^s - \mu_1^0}{k_b T}, \quad (1-11)$$

in which the approximation $V \gg N_a$ is used. The free energy has an extremum in $x_1^* < 1$, indicating that stability is achieved at $x_1^* \neq 0$. Under this condition, the criterion for PT1 is given by

$$\mu_1^s - \mu_1^0 < k_b T \ln \frac{N_a}{V}, \quad (1-12)$$

suggesting that if the interaction energy μ_1^s is low, the cell system becomes stable by forming SFs and establishing order. In other words, the system spontaneously moves towards an ordered state characterized by SF formation when substrate stiffness is high, enabling greater tension generation due to the law of action and reaction. Conversely, if μ_1^s is high, the cell is more stable when actin particles remain randomly distributed without forming SFs. While this model assumes constant cell volume and actin particle number, the result suggests that a higher effective concentration of actin particles, N_a/V , facilitates SF formation. Interestingly, even though this model does not explicitly consider the effect of concentration, its impact on the cell stability is revealed within the framework of statistical mechanics.

Using the more rigorous Eq. (1-10), we numerically show the relationship between the order parameter x_1 and the free energy A_1 (Figs. 3–5). Hereafter, unless otherwise stated, these parameters are used: $N_a = 100$, $T = 309.5$ K, $k_b = 1.38 \times 10^{-23}$ J/K, $F_1 = 1 \times 10^{-12}$, $a = 20$, $B = 1.5 \times 10^{-20}$, and $C = 2.5 \times 10^{12}$. B and C , which affect the magnitude of the energy, are determined given that the binding free energy of proteins generally falls within the range of 1–10 kcal/mol (19). Under conditions where the tension F_1 is small, the free energy A_1 reaches its minimum at $x_1 = 0$ (Fig. 3, blue and orange), indicating that the cell system is stable in a disordered state where actin particles are randomly distributed without forming SFs. Once F_1 exceeds a certain threshold, A_1 shifts to its minimum at higher values of x_1 (Fig. 3, green and red), suggesting that in environments with larger forces, such as those with greater substrate stiffness, the cell system is more stable as it adopts an ordered phase characterized by the presence of one or more SFs. In environments where the total number of effective actin particles N_a is small, the free energy A_1 reaches its minimum at $x_1 = 0$ (Fig. 6a, blue), suggesting that the cell system is stable in a state where actin particles are randomly distributed. As N_a increases, in contrast, the free energy minimum shifts to a larger value of x_1 (Fig. 6a, green and red), indicating that cells with higher actin concentrations are more stable in an ordered phase where SFs are formed (Figs. 6b and 7). The analytical results for the order parameter x_1^* , at which the free energy is minimized, also demonstrate a similar phase transition as in the numerical analysis (data not shown).

Phase transition 2

We explore the mechanism of the phase transition from a cell structure with SFs formed in random directions to one where SFs acquire a specific orientation, characteristic of Phase transition 2 (PT2). In the previous phase, the presence of SFs alone was regarded as an ordered state. In contrast, PT2 is interpreted as the emergence of a new order, where SFs align in a particular direction. In this new phase, SFs align either vertically or horizontally (Fig. 8). Although in actual cells not all actin particles form SFs, we consider that the cell is entirely in an SF-forming phase to focus on the essential aspects of this specific phase transition. In addition, while actual SFs can align in various directions, we count only those aligning vertically or horizontally. Note that if a more rigorous model is required with a wider range of SF orientations, the methodology for counting entropy and energy can be accordingly expanded to accommodate this.

Within the square lattice framework as used for PT1, let us consider the case where the total number of SFs is n_2 . We denote the number of SFs aligning along the x -axis as n_2^x (Fig. 8, green) and those aligning along the y -axis as n_2^y (orange), and thus

$$n_2 = n_2^x + n_2^y \quad (2 - 1)$$

The new order parameter that determines the phase state here is defined as follows to evaluate the extent to which SFs are aligned in the same specific directions.

$$x_2 = \frac{n_2^x - n_2^y}{n_2} \quad (2 - 2)$$

When $x_2 = 0$, SFs are evenly distributed between the two axes, indicating a disordered state; meanwhile, when $x_2 = 1$ or $x_2 = -1$, SFs are aligned only along either the x -axis or y -axis, reflecting a state with directional order. The number of possible microstates is described by

$$W = \frac{n_2!}{n_2^x! n_2^y!}, \quad (2 - 3)$$

and then the entropy is described, with the Stirling approximation, by

$$\begin{aligned} S_2 &= k_b \ln W \\ &= k_b \left(n_2 \ln n_2 - \frac{1+x_2}{2} \ln \left(\frac{1+x_2}{2} n_2 \right) - \frac{1-x_2}{2} \ln \left(\frac{1-x_2}{2} n_2 \right) \right) \end{aligned} \quad (2 - 4)$$

(Fig. S3). We define the energy of a single SF bearing a tension of F_2 based on the catch-bond properties:

$$\mu_2(F_2) = \mu_2^0 \exp\left(-\frac{F_2}{F_2^0}\right), \quad (2 - 5)$$

in which F_2 ($= f_2 a$) is the maximum tension that fully formed single SFs can generate; f_2 is the unit tension, F_2^0 is a normalizing factor, and a is the cell edge length as in PT1. Tension in proliferative cells is known to be produced by the interaction between ubiquitous nonmuscle actin and myosin II filaments, which occurs when these proteins align in a straight configuration (20,21). Based on this, we assume that when one SF crosses another perpendicularly, the intersection point lacks the linear structure effective for tension production. If an SF does not experience such interference from others, the tension it can generate reaches its maximum value of F_2 . The tensions in the x -axis and y -axis directions

are then given as follows:

$$\begin{aligned} F_2^y &= f_2(a - n_2^x) \\ F_2^x &= f_2(a - n_2^y) \end{aligned} \quad (2-6)$$

From Eqs. (2-4) and (2-5), the energy E_2 and free energy A_2 are given by:

$$E_2 = n_2^y \mu_2(F_2^y) + n_2^x \mu_2(F_2^x) \quad (2-7)$$

(Fig. S4) and

$$\begin{aligned} A_2 = \mu_2^0 \left\{ \frac{1-x_2}{2} n_2 \mu_2^0 \exp\left(-\frac{f_2\left(a - \frac{(1+x_2)n_2}{2}\right)}{F_2^0}\right) + \frac{1+x_2}{2} n_2 \mu_2^0 \exp\left(-\frac{f_2\left(a - \frac{(1-x_2)n_2}{2}\right)}{F_2^0}\right) \right\} \\ - T k_b \left(n_2 \ln n_2 - \frac{1+x_2}{2} \ln\left(\frac{1+x_2}{2} n_2\right) - \frac{1-x_2}{2} \ln\left(\frac{1-x_2}{2} n_2\right) \right), \end{aligned} \quad (2-8)$$

respectively. To analyze the critical condition, taking the second derivative of Eq. (2-8) with respect to x_2 and substituting $x_2 = 0$ yield

$$\frac{\partial^2 A_2(0)}{\partial x_2^2} = \frac{n_2^2 f_2 \mu_2^0}{4 F_2^0} \left(-4 + \frac{f_2 n_2}{F_2^0} \right) \exp\left(-\frac{f_2\left(a - \frac{n_2}{2}\right)}{F_2^0}\right) + T k_b. \quad (2-9)$$

With the approximation $f_2\left(a - \frac{n_2}{2}\right)/F_2^0 \ll 1$ and solving $\partial^2 A_2(0)/\partial x_2^2 = 0$,

$$f_2^* = \frac{2\left(F_1^0 \mu_2^0 n_2 - F_2^0 \sqrt{\mu_2^{02} n_2^2 - k_b \mu_2^0 n_2^2 T}\right)}{\mu_0 n^2}, \quad (2-10)$$

and thus the cell system stabilizes at $x_2 = 0$ when $f_2 < f_2^*$, and at $x_2 \neq 0$ when $f_2 > f_2^*$.

Using the rigorous Eq. (2-8) with $\mu_2^0 = 10^{-20}$, $F_2^0 = 10^{-9}$, and $n_2 = 100$, we visualized the relationship between the free energy A_2 and the order parameter x_2 (Fig. 9a, blue and orange), showing that A_2 reaches its minimum at $x_2 = 0$ when the force f_2 is small. Meanwhile, the free energy has a convex shape and reaches its minimum at $x_2 \neq 0$ when

the force is large (Fig. 9a, green). Thus, SFs sustaining low tension remain stable with random orientation, but once the tension exceeds a certain threshold the influence of energy becomes more dominant than entropy, leading to a phase where SFs align in a consistent direction (Fig. 9b, c). When the total number of distinct SFs, n_2 , is small, the order parameter corresponding to the minimum free energy begins to change at higher force levels (Fig. 10). In contrast, when n_2 is large, the change in the order parameter starts at lower force levels, suggesting that PT2 occurs more easily with more SFs under the same force conditions than with fewer SFs.

Phase transition 3

Next, we focus on the mechanism of Phase transition 3 (PT3) in which SFs, after acquiring directional alignment in PT2, undergo further transformation to undergo interfiber coupling. As in the previous sections, we consider a simple model where directionally aligned SFs are distributed within a square cell lattice of side length a with constant volume and temperature (Fig. 11). In actual cells, not all SFs align in a single direction, but we focus on the key aspects of how directionally aligned SFs cluster after PT2. Let the total number of SFs be n_3 , and let n_3^{SF} and n_3^{ass} represent the number of independent and assembled ones, respectively:

$$n_3 = n_3^{SF} + n_3^{ass} \quad (3 - 1)$$

We consider the case where a single aggregate is present. Although multiple aggregates form in actual cells, this complexity can be addressed by adjusting entropy calculations. Here, however, the focus is on establishing a framework for analyzing the fundamental principles and significance of PT3. The order parameter is defined as follows to evaluate the extent to which SFs form aggregates:

$$x_3 = \frac{n_3^{ass}}{n_3} \quad (3 - 2)$$

SFs are independently distributed at $x_3 = 0$, reflecting a disordered state, while they undergo interfiber coalescence at $x_3 = 1$. The number of microstates is expressed as follows, focusing on the distribution patterns:

$$W = \frac{(a + 1 - n_3^{ass})!}{(n_3 - n_3^{ass})! (a - n_3^{ass})!} \quad (3 - 3)$$

The entropy is described, with the Stirling approximation, by

$$S_3 = k_b \ln W$$

$$= k_b \{(a + 1 - n_3 x_3) \ln(a + 1 - n_3 x_3) - n_3(1 - x_3) \ln n_3(1 - x_3) - (a - n_3) \ln(a - n_3)\} \quad (3 - 4)$$

(Fig. S5). The energy of individual SFs is given by Eq. (2-5) as used in PT2,

$$\mu_3 = \mu_3^0 \exp\left(-\frac{c f_3}{F_3^0}\right), \quad (3 - 5)$$

but the interpretation here is that c is a concentration-dependent parameter of binding proteins such as α -actinin that stabilize the connections between SFs. The energy and free energy are then be expressed by

$$E_3 = n_3 \left\{ (1 - x_3) \mu_3^0 \exp\left(-\frac{c_{SF} f_3}{F_3^0}\right) + x_3 \mu_3^0 \exp\left(-\frac{c_{ass} f_3}{F_3^0}\right) \right\} \quad (3 - 6)$$

(Fig. S6), and

$$A_3 = n_3 \left\{ (1 - x_3) \mu_3^0 \exp\left(-\frac{c_{SF} f_3}{F_3^0}\right) + x_3 \mu_3^0 \exp\left(-\frac{c_{ass} f_3}{F_3^0}\right) \right\}$$

$$- T k_b \{(a + 1 - n_3 x_3) \ln(a + 1 - n_3 x_3) - n_3(1 - x_3) \ln n_3(1 - x_3) - (a - n_3) \ln(a - n_3)\}, \quad (3 - 7)$$

respectively, where c_{SF} and c_{ass} are c for independently distributed SFs and assembled SFs, respectively. To Differentiating Eq. (3-7) with respect to x_3 is

$$\frac{\partial A_3}{\partial x_3} = n_3 \left(-\mu_3^0 \exp\left(-\frac{c_{ass} f_3}{F_3^0}\right) + \mu_3^0 \exp\left(-\frac{c_{SF} f_3}{F_3^0}\right) \right) - T k_b (\ln(a + 1 - n_3 x_3) + \ln(n_3 - n_3 x_3)), \quad (3 - 8)$$

and the order parameter at $\partial A_3 / \partial x_3 = 0$ is expressed as

$$x_3^* = \frac{(a + 1) \exp\left(\frac{-\mu_3^0 \exp\left(-\frac{c_{ass} f_3}{F_3^0}\right) + \mu_3^0 \exp\left(-\frac{c_{SF} f_3}{F_3^0}\right)}{T k_b}\right) - n_3}{n_3 \left(\exp\left(\frac{-\mu_3^0 \exp\left(-\frac{c_{ass} f_3}{F_3^0}\right) + \mu_3^0 \exp\left(-\frac{c_{SF} f_3}{F_3^0}\right)}{T k_b}\right) - 1 \right)}. \quad (3 - 9)$$

The free energy reaches an extremum and stabilizes at this specific $x_3^* < 1$, as long as x_3^* is not equal to 0. The condition for PT3 is now described by

$$-\mu_3^0 \exp\left(-\frac{c_{ass}f_3}{F_3^0}\right) + \mu_3^0 \exp\left(-\frac{c_{SF}f_3}{F_3^0}\right) < T k_b \ln \frac{n_3}{a+1}, \quad (3-10)$$

indicating that even when the energy difference on the left side remains unchanged, PT3 can still occur if the total number of SFs is high.

Visualization of PT3 with $n_3 = 100$ and $F_3^0 = 1 \times 10^{-9}$ shows that entropy dominates when the tension is weak with a low binding protein concentration, leading to a state where the free energy is minimized at $x_3 = 0$ (Fig. 12a, blue and orange). On the other hand, a high binding protein concentration leads to stabilization of the cell system with SF aggregates (Fig. 12a, green). One straightforward interpretation of the parameter c_{ass} is the concentration of actin binding proteins that allow SFs to engage in interfiber coupling, but another is that c_{ass} also represents the internal and external factors that drive changes in the size of SFs through the enlargement of focal adhesions and consequently increase the sustained tension, which is also enhanced by substrate stiffness (Fig. 12b, c) (22–26). The threshold concentration decreases as the total number of SFs increases (Fig. 13). This observation is consistent with the theoretically derived phase transition conditions (Eqs. (3-9) and (3-10)).

Discussion

This study provides a novel thermodynamic perspective on the adaptive structural changes in living cells, particularly focusing on the formation and organization of SFs in direct accordance with environmental stiffness. While previous research has extensively explored the dynamics of cellular components (8,27–29), these studies often depend on specific experimental and numerical parameters, making it challenging to achieve a unified understanding of the universal features. In contrast, our approach clarifies the underlying physical principles that govern environment-dependent intracellular phase transitions. Our findings reveal that the stepwise transitions observed in SF formation are not merely stochastic but are driven by a delicate balance between energy and entropy, inherently dictated by substrate stiffness.

A key contribution of this study is the identification of distinct phase transitions as cells

respond to varying degrees of substrate stiffness. These transitions, characterized by the emergence and specific alignment of SFs, share similarities with the way phase transitions are understood in condensed matter physics. Thus, we employed a statistical mechanics approach to decipher the conditions that make these biological transitions energetically favorable. Our findings suggest that cellular phase transitions are influenced not only by external mechanical cues but also by internal parameters such as effective actin concentration and SF interactions.

These phase transitions have implications beyond structural stability. When cells fail to maintain a stable phase, especially when SFs cannot properly form or align under mechanical stress, they may enter a pro-inflammatory state, potentially leading to chronic inflammatory diseases like atherosclerosis (30–32). Focal adhesions at SF termini convert mechanical tension into biochemical signals, with insufficient tension leading to sustained activation of pathways such as MAPK and subsequent disease progression (33,34). While previous studies have explored tension-dependent stability of focal adhesions and SFs at the molecular level (35,36), our study provides a cell-level perspective on how overall cellular stability is achieved in response to surrounding cues.

The continuous phase transitions observed during spreading of cells plated on stiffer substrates can be understood as the sequential internal stiffening of the cell. This process is driven by intracellular percolation (23), where actin–myosin interactions progressively form SFs that facilitate increased tension generation, reflecting the gradual rise in intracellular stiffness. This dynamic adaptation highlights the flexibility of cells in responding to internal and external cues, allowing them to reorganize their structures and maintain stability across various conditions. The cell cycle is precisely regulated by biochemical checkpoints such as cyclins and cyclin-dependent kinases, which ensure accurate progression through each phase. During the G1 phase, cells attach to the substrate and begin spreading, a process supported by the gradual formation of SFs, preparing the cell for subsequent phases. Our study suggests that, in addition to these biochemical checkpoints, “mechanical” checkpoints exist during the G1 phase, regulating the formation of intracellular structures and associated signaling to further ensure proper cell cycle progression.

Our thermodynamic understanding offers a comprehensive framework that not only explains the stepwise phase transitions in SF organization but also provides insights into the broader mechanisms of cellular adaptation. By considering the interplay between energy and entropy, we have identified the critical physical relationships that govern these spontaneous adaptations, demonstrating that the process is complex yet inherently deterministic, driven by both internal and external conditions of the cell. While our model focuses on the actin cytoskeleton within a two-dimensional lattice framework, it lays a solid foundation for future

research. Extending this model, for example, to include additional cellular components, higher-dimensional lattices, or curved SF arrangements could yield more accurate representations of cellular phenomena. Although such detailed modeling is beyond the scope of this study, our work provides a foundational framework upon which future research can build. As phase transitions involving environment-dependent shifts in stability are a fundamental concept in physics, the principles outlined here may offer valuable insights into the complexity of biological adaptation.

Acknowledgments

Y.U. is supported by the Japan Society for the Promotion of Science (JSPS). This study was supported in part by JSPS KAKENHI grants (23H04929 and 24KJ1649).

References

1. Discher DE, Janmey P, Wang YL. Tissue cells feel and respond to the stiffness of their substrate. *Science*. 2005 Nov 18;310(5751):1139–43.
2. Prager-Khoutorsky M, Lichtenstein A, Krishnan R, Rajendran K, Mayo A, Kam Z, et al. Fibroblast polarization is a matrix-rigidity-dependent process controlled by focal adhesion mechanosensing. *Nat Cell Biol*. 2011;13.
3. Friedrich BM, Buxboim A, Discher DE, Safran SA. Striated Acto-Myosin Fibers Can Reorganize and Register in Response to Elastic Interactions with the Matrix. *Biophys J*. 2011 Jun 8;100(11):2706–15.
4. Greiner AM, Chen H, Spatz JP, Kemkemer R. Cyclic Tensile Strain Controls Cell Shape and Directs Actin Stress Fiber Formation and Focal Adhesion Alignment in Spreading Cells. *PLoS One*. 2013 Oct 28;8(10):e77328.
5. McGrath JL. Cell Spreading: The Power to Simplify. *Current Biology*. 2007 May 15;17(10):R357–8.
6. Ladoux B, Mège RM, Trepas X. Front–Rear Polarization by Mechanical Cues: From Single Cells to Tissues. *Trends Cell Biol*. 2016 Jun 1;26(6):420–33.

7. Thompson CJ. The statistical mechanics of phase transitions. *Contemp Phys.* 1978;19(3):203–24.
8. Prager-Khoutorsky M, Lichtenstein A, Krishnan R, Rajendran K, Mayo A, Kam Z, et al. Fibroblast polarization is a matrix-rigidity-dependent process controlled by focal adhesion mechanosensing. *Nat Cell Biol.* 2011 Dec;13(12):1457–65.
9. Valle-Orero J, Eckels EC, Stirnemann G, Popa I, Berkovich R, Fernandez JM. The elastic free energy of a tandem modular protein under force. *Biochem Biophys Res Commun.* 2015 May 1;460(2):434–8.
10. Frederick KK, Marlow MS, Valentine KG, Wand AJ. Conformational entropy in molecular recognition by proteins. *Nature* 2007 448:7151. 2007 Jul 19;448(7151):325–9.
11. Chen AL, Liang TL. Nonlinear dynamics and statistical physics of DNA You may also like Band structures of elastic waves in two-dimensional eight-fold solid-solid quasi-periodic phononic crystals. 2004;
12. Pande VS, Grosberg AY, Tanaka T. Statistical mechanics of simple models of protein folding and design. *Biophys J.* 1997 Dec 1;73(6):3192–210.
13. Ueda Y, Matsunaga D, Deguchi S. A statistical mechanics model for determining the length distribution of actin filaments under cellular tensional homeostasis. *Scientific Reports* 2022 12:1. 2022 Aug 24;12(1):1–10.
14. Nishizaka T, Seo R, Tadakuma H, Kinosita K, Ishiwata S. Characterization of single actomyosin rigor bonds: Load dependence of lifetime and mechanical properties. *Biophys J.* 2000 Aug 1;79(2):962–74.
15. Akalp U, Schnatwinkel C, Stoykovich MP, Bryant SJ, Vernerey FJ. Structural Modeling of Mechanosensitivity in Non-Muscle Cells: Multiscale Approach to Understand Cell Sensing. *ACS Biomater Sci Eng.* 2017 Nov 13;3(11):2934–42.
16. Thomas W. For catch bonds, it all hinges on the interdomain region. *Journal of Cell Biology.* 2006 Sep 25;174(7):911–3.

17. Guo B, Guilford WH. Mechanics of actomyosin bonds in different nucleotide states are tuned to muscle contraction. *Proc Natl Acad Sci U S A*. 2006 Jun 27;103(26):9844–9.
18. Inoue Y, Adachi T. Role of the actin-myosin catch bond on actomyosin aggregate formation. *Cell Mol Bioeng*. 2013 Mar 27;6(1):3–12.
19. Vreven T, Hwang H, Pierce BG, Weng Z. Prediction of protein-protein binding free energies. *Protein Science*. 2012 Mar;21(3):396–404.
20. Huang W, Matsui TS, Saito T, Kuragano M, Takahashi M, Kawahara T, et al. Mechanosensitive myosin II but not cofilin primarily contributes to cyclic cell stretch-induced selective disassembly of actin stress fibers. *Am J Physiol Cell Physiol*. 2021 Jun 1;320(6):C1153–63.
21. Matsui TS, Deguchi S. Spatially selective myosin regulatory light chain regulation is absent in dedifferentiated vascular smooth muscle cells but is partially induced by fibronectin and Klf4. *Am J Physiol Cell Physiol*. 2019 Apr 1;316(4):C509–21.
22. Goffin JM, Pittet P, Csucs G, Lussi JW, Meister JJ, Hinz B. Focal adhesion size controls tension-dependent recruitment of α -smooth muscle actin to stress fibers. *Journal of Cell Biology*. 2006 Jan 16;172(2):259–68.
23. Ueda Y, Matsunaga D, Deguchi S. Asymmetric response emerges between creation and disintegration of force-bearing subcellular structures as revealed by percolation analysis. *Integrative Biology*. 2024 Jan 23;16.
24. Wolfenson H, Bershadsky A, Henis YI, Geiger B. Actomyosin-generated tension controls the molecular kinetics of focal adhesions. *J Cell Sci*. 2011 May 1;124(9):1425–32.
25. Ren XD, Kiosses WB, Schwartz MA. Regulation of the small GTP-binding protein Rho by cell adhesion and the cytoskeleton. *EMBO Journal*. 1999 Feb 1;18(3):578–85.
26. Cao X, Lin Y, Driscoll TP, Franco-Barraza J, Cukierman E, Mauck RL, et al. A Chemo-Mechanical Model for Extracellular Matrix and Nuclear Rigidity Regulated Size of Focal Adhesion Plaques. *Biophys J*. 2016 Feb 16;110(3):622a.
27. Trichet L, Le Digabel J, Hawkins RJ, Vedula RK, Gupta M, Ribault C, et al. Evidence of a

large-scale mechanosensing mechanism for cellular adaptation to substrate stiffness. *SCIENCES BIOPHYSICS AND COMPUTATIONAL BIOLOGY*. 2012;109(18).

28. Ibata N, Terentjev EM. Development of Nascent Focal Adhesions in Spreading Cells. *Biophys J*. 2020 Nov 17;119(10):2063–73.
29. Senju Y, Miyata H. The role of actomyosin contractility in the formation and dynamics of actin bundles during fibroblast spreading. *J Biochem*. 2009 Feb;145(2):137–50.
30. Hahn C, Schwartz MA. Mechanotransduction in vascular physiology and atherogenesis. *Nature Reviews Molecular Cell Biology* 2009 10:1. 2009 Jan;10(1):53–62.
31. Humphrey JD, Schwartz MA. Vascular Mechanobiology: Homeostasis, Adaptation, and Disease. *Annu Rev Biomed Eng*. 2021;23(1):1–27.
32. Chien S. Mechanotransduction and endothelial cell homeostasis: The wisdom of the cell. *Am J Physiol Heart Circ Physiol*. 2007 Mar;292(3):1209–24.
33. Kaunas R, Deguchi S. Multiple Roles for Myosin II in Tensional Homeostasis Under Mechanical Loading.
34. Deguchi S, Matsui TS, Iio K. The position and size of individual focal adhesions are determined by intracellular stress-dependent positive regulation. *Cytoskeleton*. 2011 Nov;68(11):639–51.
35. Deshpande VS, McMeeking RM, Evans AG. A bio-chemo-mechanical model for cell contractility. *Proc Natl Acad Sci U S A*. 2006 Sep 19;103(38):14015–20.
36. Olberding JE, Thouless MD, Arruda EM, Garikipati K. The Non-Equilibrium Thermodynamics and Kinetics of Focal Adhesion Dynamics. *PLoS One*. 2010 Aug 18;5(8):e12043.

Figures

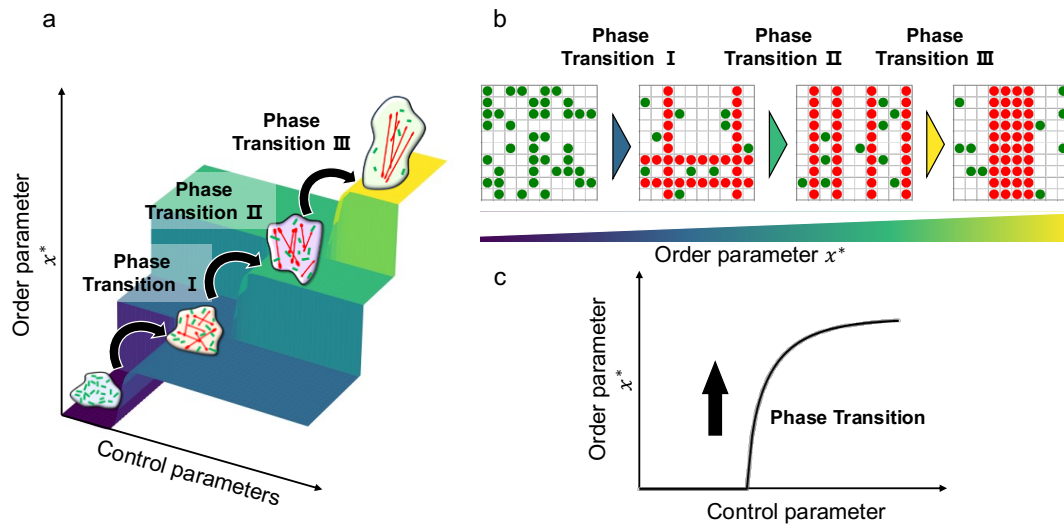


Fig. 1 Overview of cellular stepwise transitions. (a) Phase transitions in the internal actin structures occur step by step in accordance with control parameters including substrate stiffness. (b) Cell lattice models to analyze each of the phase transitions. Initially, randomly distributed actin particles (green) create long filaments (red) (I), align in the same direction (II), and eventually achieve interfiber coupling (III) as a function of the order parameter. (c) Schematic illustrating the phase transition, where the order parameter changes discontinuously at a critical control parameter.

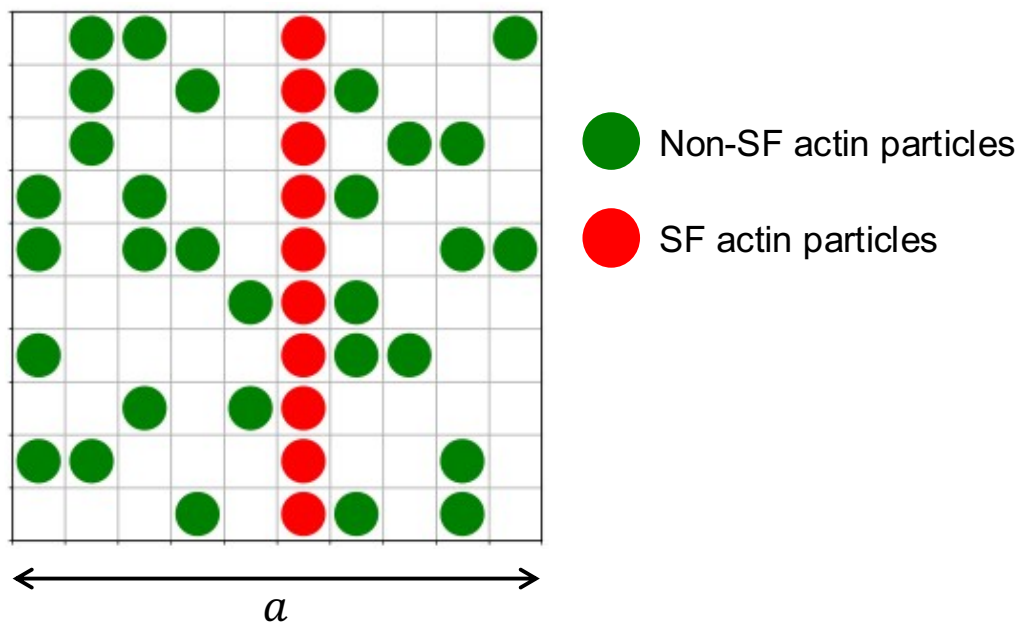


Fig. 2 Schematic of a cell lattice model for PT1. Actin particles are distributed and consist of two types: non-SF actin particles (green) and SF actin particles (red).

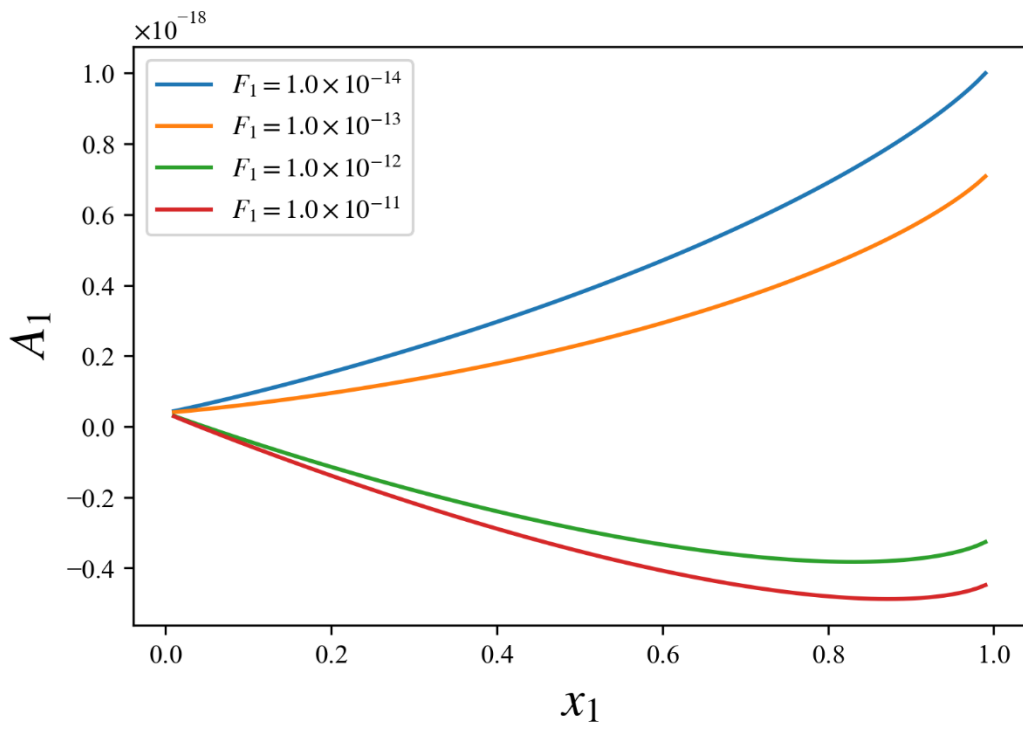


Fig. 3 Free energy as a function of the order parameter and sustained tension.

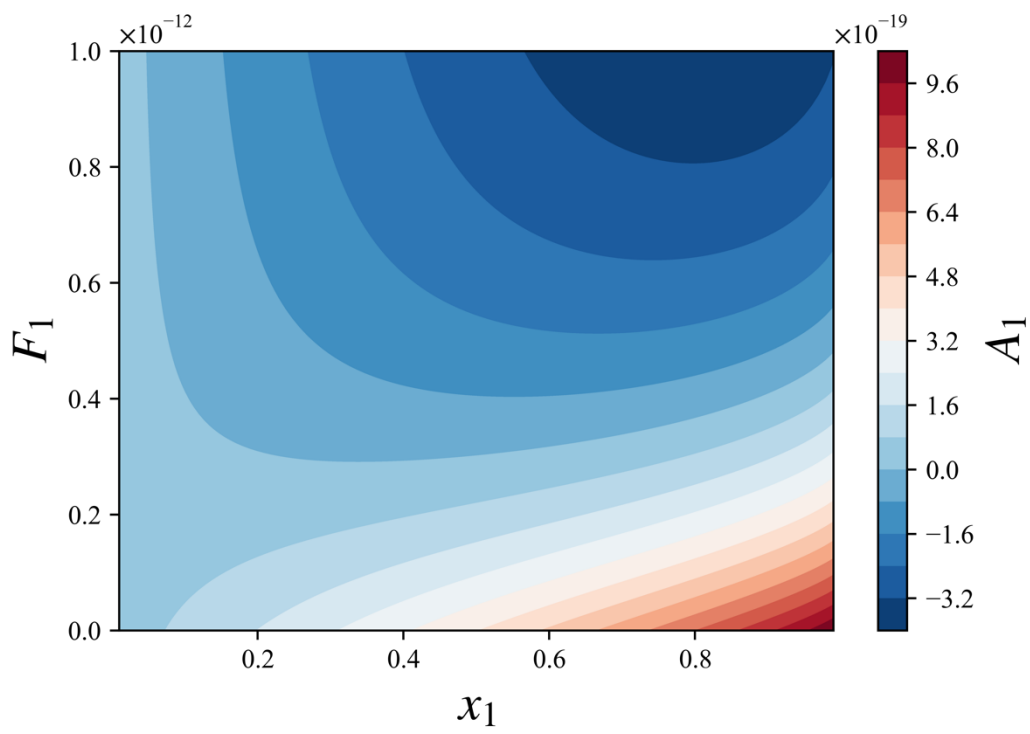


Fig. 4 Map of free energy as a function of the order parameter and sustained tension.

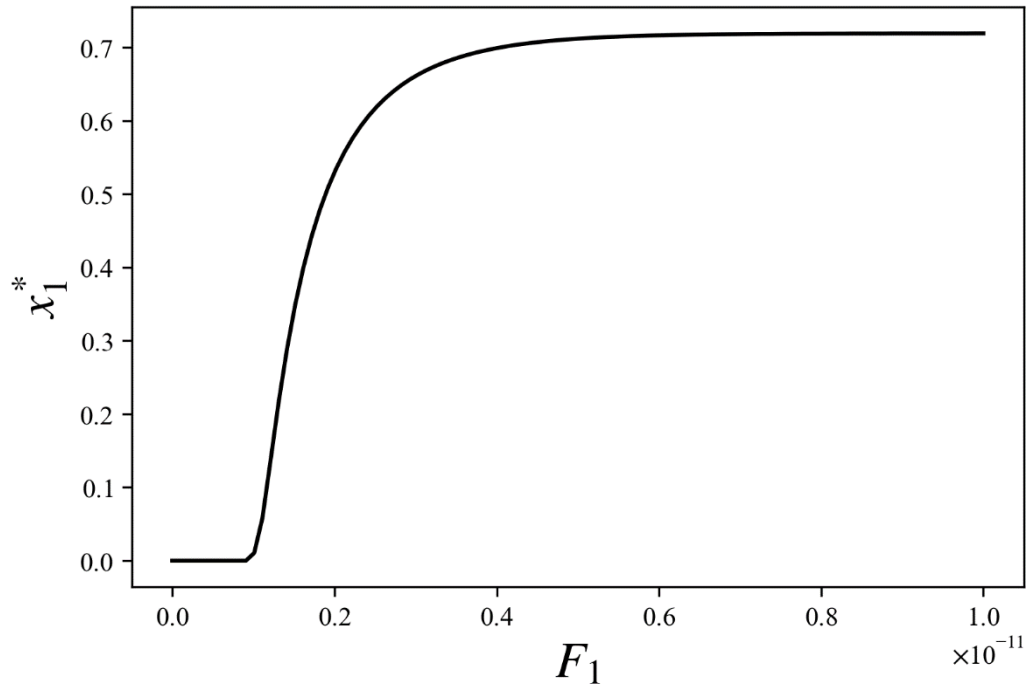


Fig. 5 Order parameter corresponding to the minimum free energy as a function of the sustained tension.

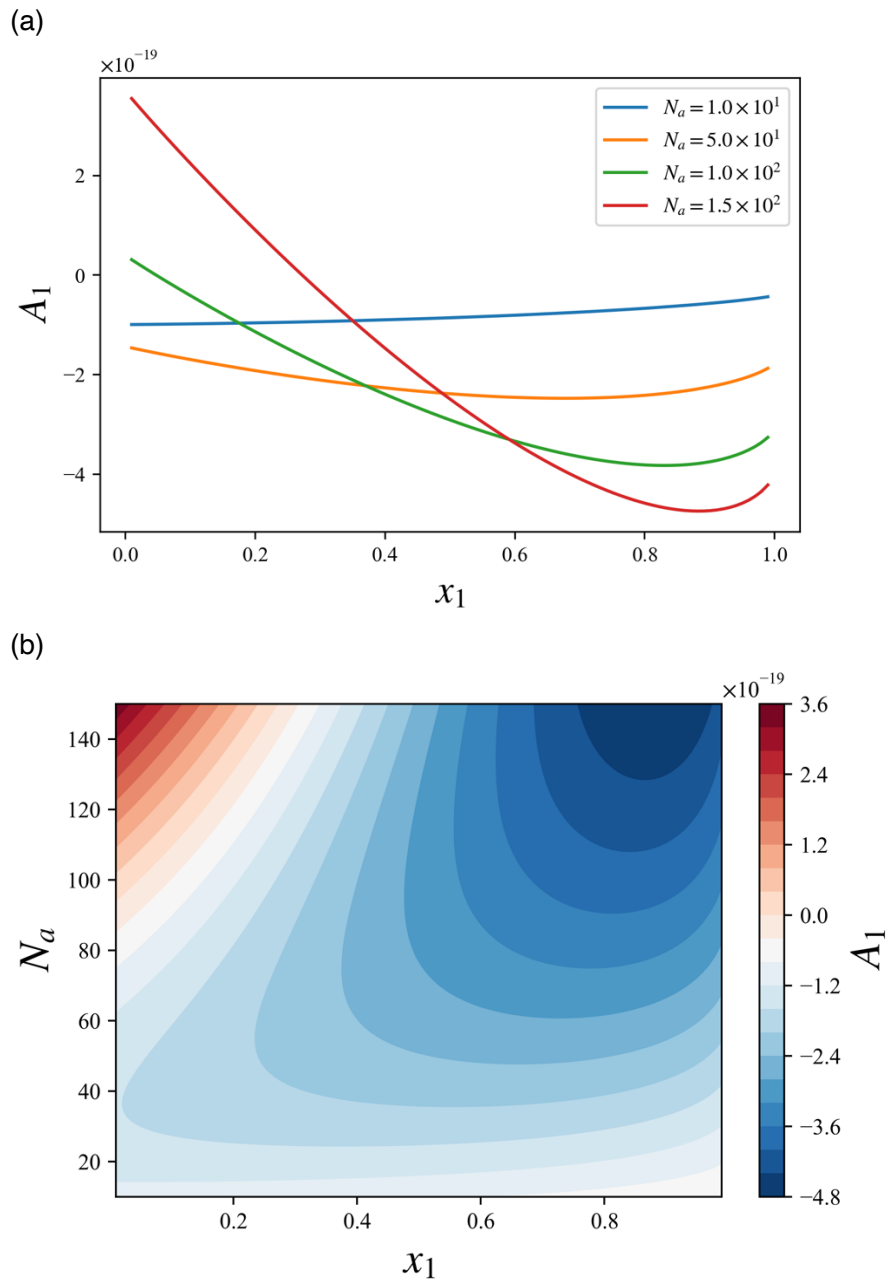


Fig. 6 The effect of effective actin concentration. (a) Free energy as a function of the order parameter and actin concentration. (b) Map of free energy as a function of the order parameter and actin concentration.

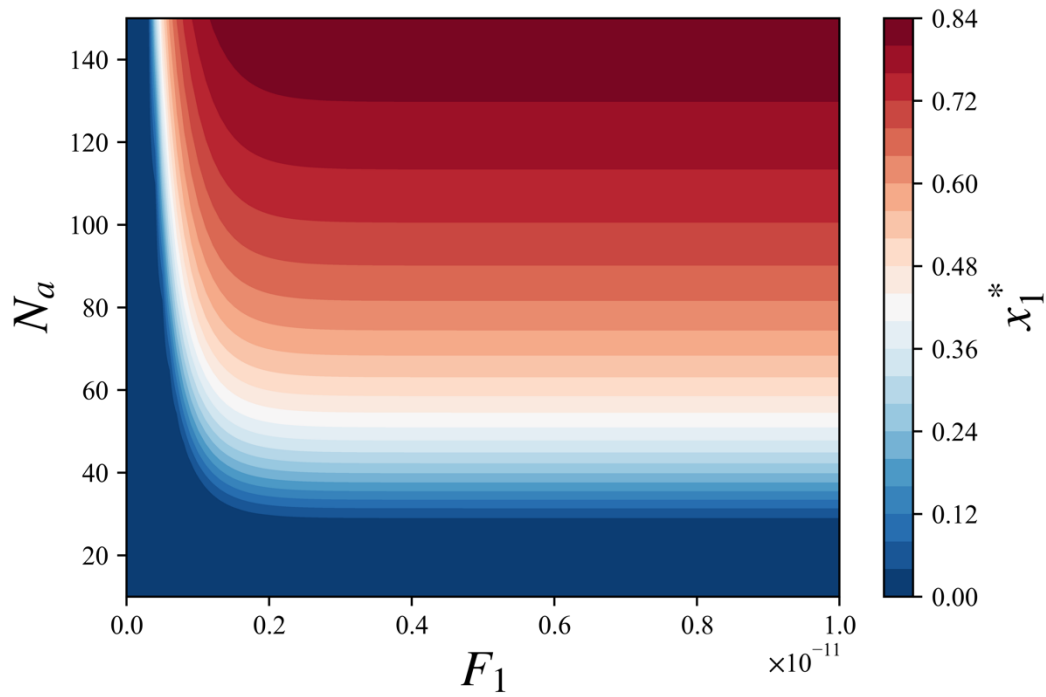


Fig. 7 Critical order parameter as a function of the effective actin concentration and sustained tension.

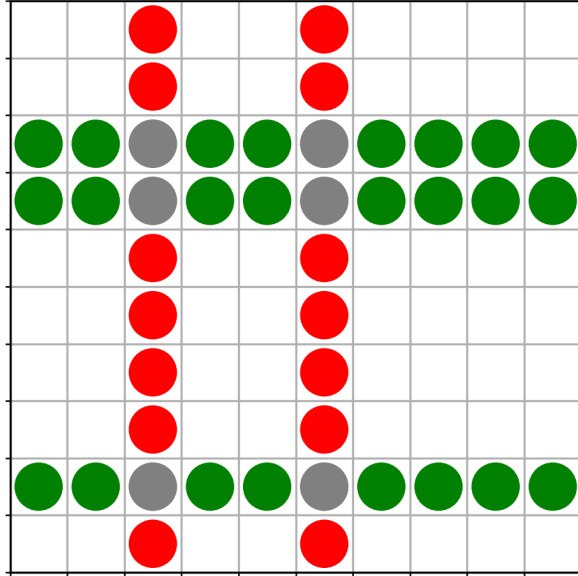


Fig. 8 Schematic of a cell lattice model for PT2. Actin particles align in the x -axis (green) or y -axis (red) to form SFs, in which the tension generation is abrogated at the intersection (gray).

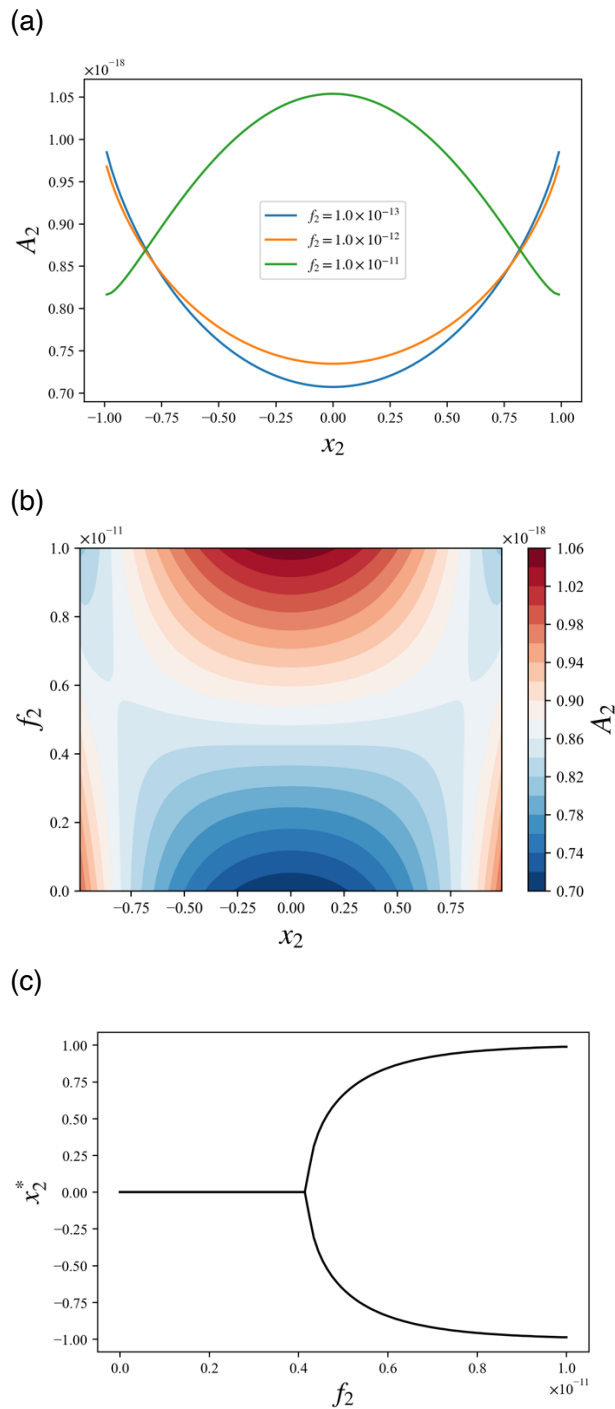


Fig. 9 The behavior of PT2. (a) Free energy as a function of the order parameter and sustained tension. (b) Map of free energy as a function of the order parameter and sustained tension. (c) Order parameter corresponding to the minimum free energy as a function of the sustained tension.

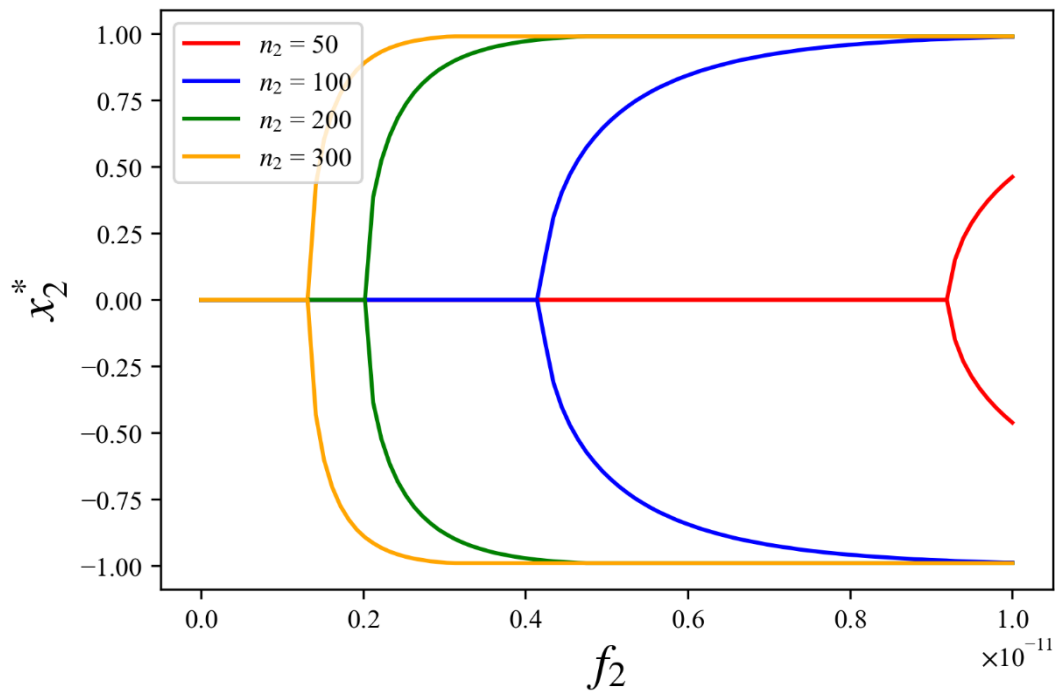


Fig. 10 Order parameter corresponding to the minimum free energy as a function of the total number of actin particles and sustained tension.

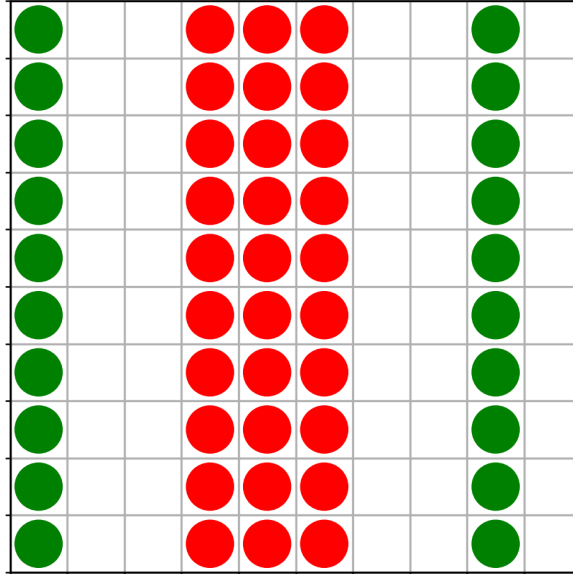


Fig. 11 Schematic of a cell lattice model for PT3. Directionally aligned SFs are either distributed independently (green) or organized into assembled structures (red).

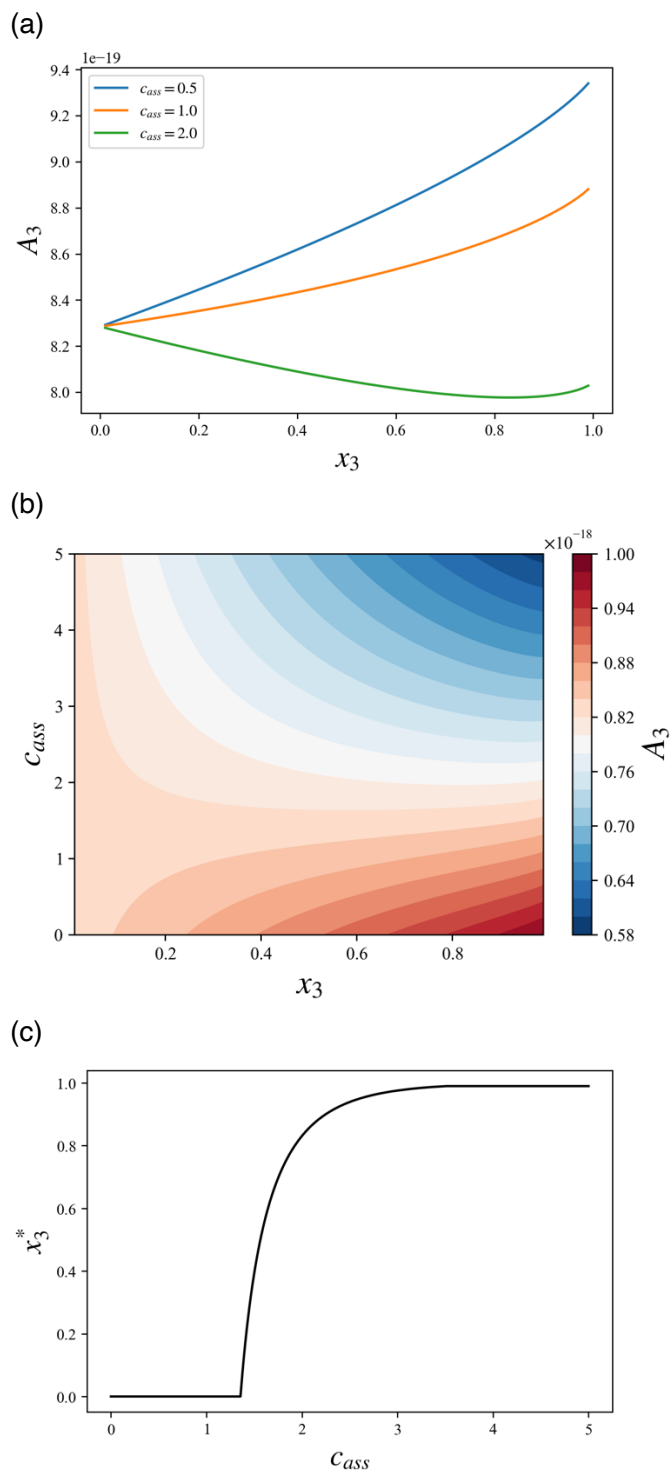


Fig. 12 The behavior of PT3. (a) Free energy as a function of the order parameter and effective binding protein concentration. (b) Map of free energy as a function of the order parameter and binding protein concentration. (c) Order parameter corresponding to the minimum free energy as a function of binding protein concentration.

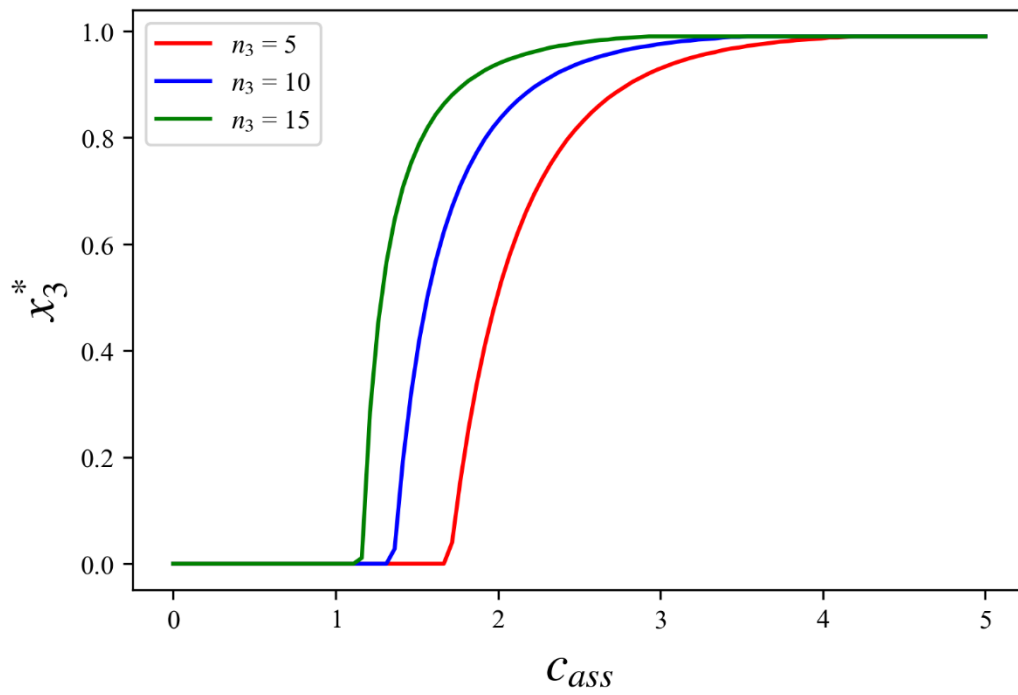


Fig. 13 Order parameter corresponding to the minimum free energy as a function of the total number of SFs and binding protein concentration.

Supplemental figures

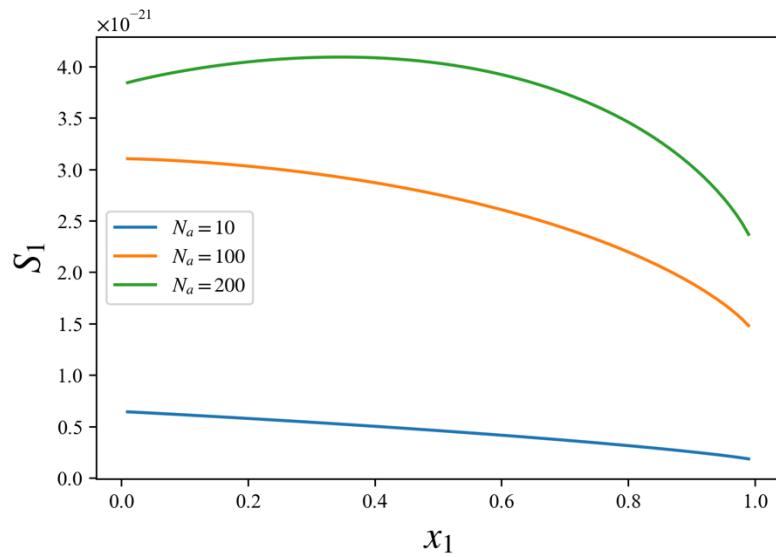


Fig. S1 Entropy vs. order parameter for PT1.

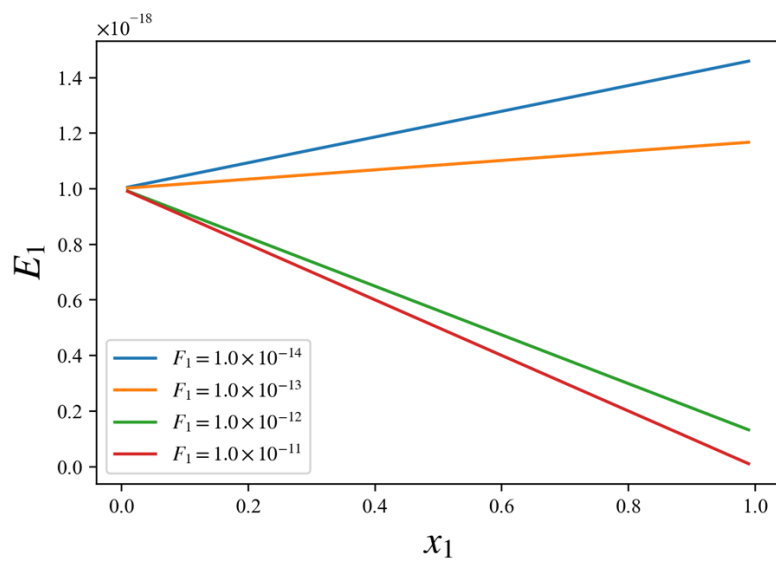


Fig. S2 Energy vs. order parameter for PT1.

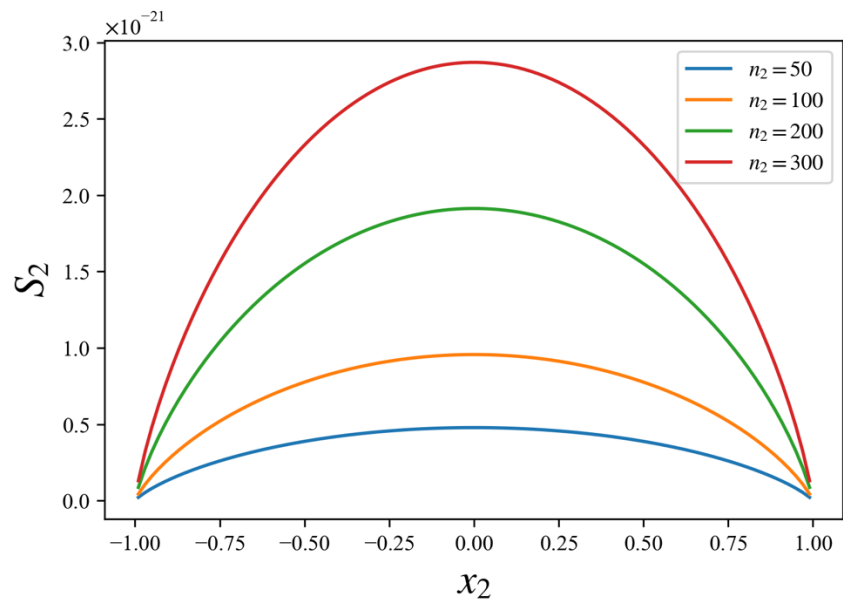


Fig. S3 Entropy vs. order parameter for PT2.

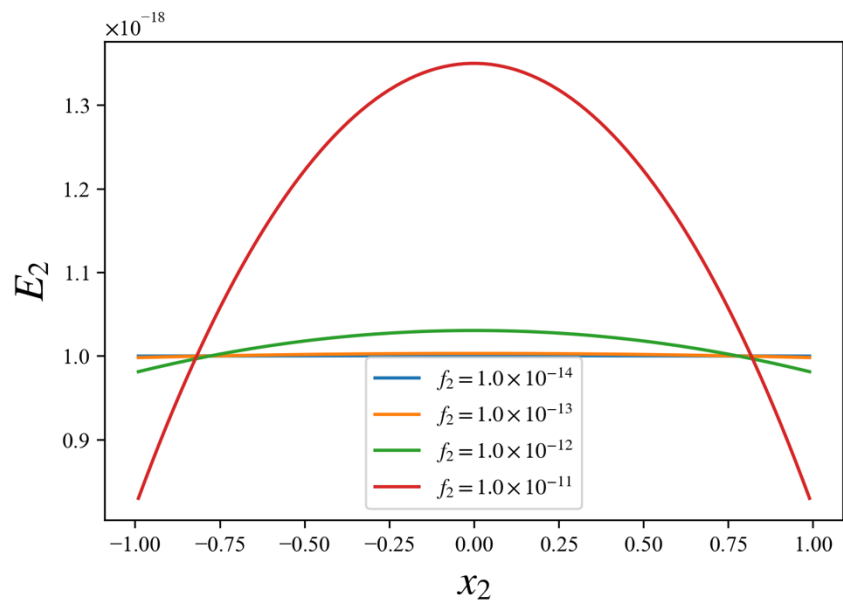


Fig. S4 Energy vs. order parameter for PT1.

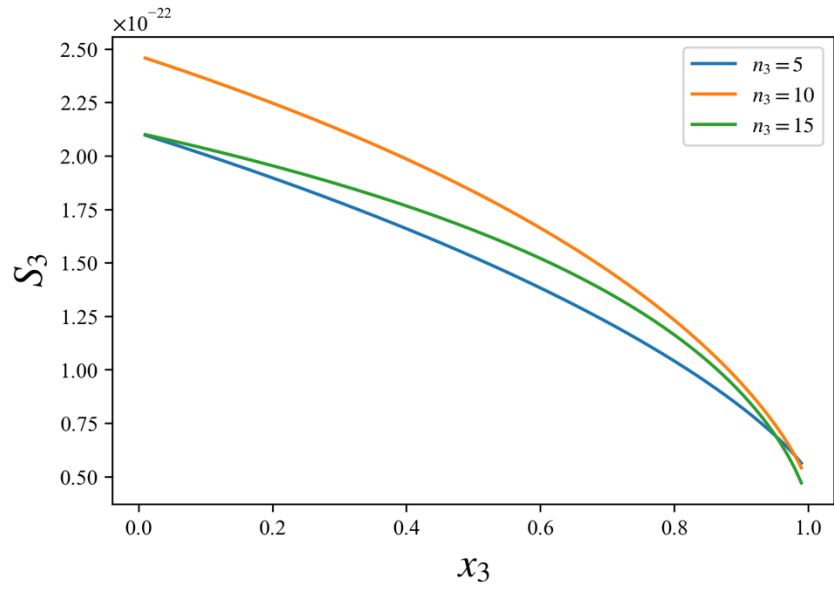


Fig. S5 Entropy vs. order parameter for PT3.

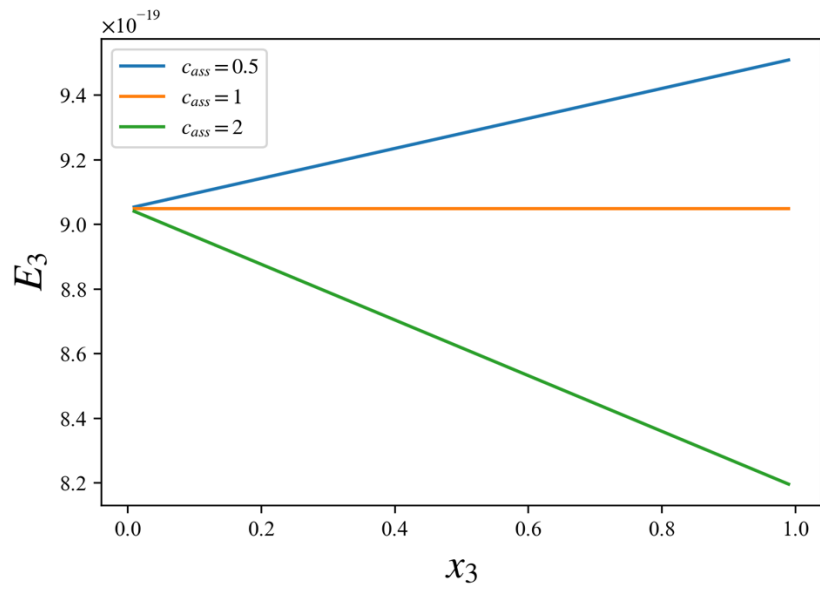


Fig. S6 Energy vs. order parameter for PT3.